Electronic Supplementary Information

for

Thermal methods usage features for multicomponent crystals screening

*Denis E. Boycov,[a] Alex N. Manin,[a] Ksenia V. Drozd,[a] Andrei V. Churakov,[b] German L. Perlovich[a]**

[a] G.A. Krestov Institute of Solution Chemistry of the Russian Academy of Sciences, 1 Akademicheskaya St., 153045, Ivanovo, Russia

[b] N.S. Kurnakov Institute of General and Inorganic Chemistry of the Russian Academy of Sciences, 31 Leninsky Prosp., 119991, Moscow, Russia

Table S1. Physicochemical characteristics of melting process of the objects of investigation

Compound	M_r, g mol^{-1}	Phase transition temperatures, °C
Nalidixic acid	232.24	227.7 ± 0.5 (fusion)[1]
Oxolinic acid	261.23	319.0 ± 0.5 (fusion with decomposition)[1]
Norfloxacin	319.33	80–117 (dehydration) 195.6 (solid-solid transition) 220.4 ± 0.2 (fusion with decomposition)[2]
Levofloxacin	361.37	50–85 (desolvation) 232.9 ± 0.2 (fusion)[2]
Enrofloxacin	359.40	221.6 ± 0.2 (fusion with decomposition)[2]
Tyramine	137.18	160-162 (fusion)[3]

1. A. N. Manin, A. P. Voronin, K. V. Drozd and G. L. Perlovich, Thermochim. Acta, 2019, 682, 178411
2. S. Blokhina, A. Sharapova, M. Ol'khovich and G. Perlovich, J. Chem. Thermodyn., 2017, 105, 37–43
3. S. Mittapalli, M. K. Chaitanya Mannava, R. Sahoo and A. Nangia, Cryst. Growth Des., 2019, 19, 219–230

Table S2. Crystallographic data for the [LFX+TYA] (1:1) Form I

Chemical formula	$C_{18}H_{28}FN_3O_4 \cdot C_8H_{12}NO$
Formula weight	507.62
Crystal system	triclinic
Space group	*P*-1
Temperature/K	298
a/Å	10.5239 (2)
b/Å	11.7151 (2)
c/Å	12.0893(2)
α/°	112.2334 (6)
β/°	110.0538 (7)
γ/°	99.0756 (7)
Volume/Å^3	1223.12

Table S3. Hydrogen bond geometry in the quinolone multicomponent crystals

Multicomponent crystal	Interaction	D···A/Å	H···A/Å	∠D–H···A/°
[NFX+TYA+MeOH] (1:1:1)	O21–H21··· O2	2.62	1.59	165.5
	$N21^{+}$–H27··· N3	2.87	1.90	170.3
	$N21^{+}$–H29···O1	2.82	2.00	139.9
	$N21^{+}$–H29···O3	2.80	2.07	130.8
	$N21^{+}$–H28···O2	3.71	2.95	138.3
	$N21^{+}$–H28···O3	2.85	1.94	160.5
	N3–H31···O21	3.14	2.24	158.9
	O18–H18···O2	2.73	1.88	179.7
[EFX+TYA+H_2O] (1:1:1)	O4–H4···O2	2.63	1.78	179.5
	$N4^{+}$–H42···O2	3.54	2.80	137.9
	$N4^{+}$–H42···O3	2.81	1.91	165.3
	$N4^{+}$–H43···O1	2.79	2.12	125.3
	$N4^{+}$–H43···O3	2.81	1.98	144.1
	O5–H51···N3	2.93	1.97	169.7
	$N4^{+}$–H41···O5	2.95	2.06	160.5
	O5–H52···O4	3.11	2.26	151.1

Table S4. Liquid-assisted grinding with different solvents experiment results

System	Solvent		
	EtOH	MeOH	H_2O
(NLD+TYA) (1:1)	[NLD+TYA] (1:1)	[NLD+TYA] (1:1)	[NLD+TYA] (1:1)
(OXL+TYA) (1:1)	OXL; TYA	OXL; TYA	OXL; TYA
(NFX+TYA) (1:1)	[NFX+TYA] (1:1)	[NFX+TYA+MeOH] (1:1:1)	[NFX+TYA+H_2O] (1:1:3)
(LFX+TYA) (1:1)	[LFX+TYA] (1:1) Form I	[LFX+TYA+MeOH] (1:1:1)	[LFX+TYA] (1:1) Form I
(EFX+TYA) (1:1)	[EFX+TYA+H_2O] (1:1:1)	[EFX+TYA+H_2O] (1:1:1); EFX; TYA	[EFX+TYA+H_2O] (1:1:1)

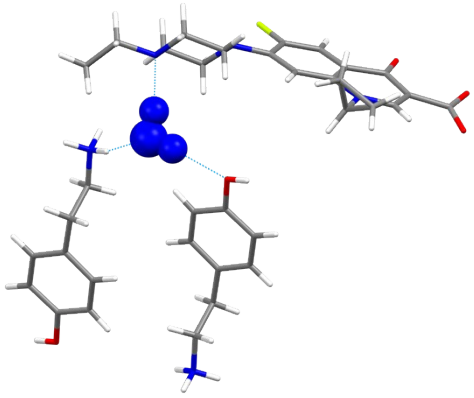

Fig. S1. Intermolecular interactions between H_2O molecules, EFX and TYA in [EFX+TYA+H_2O] (1:1:1).

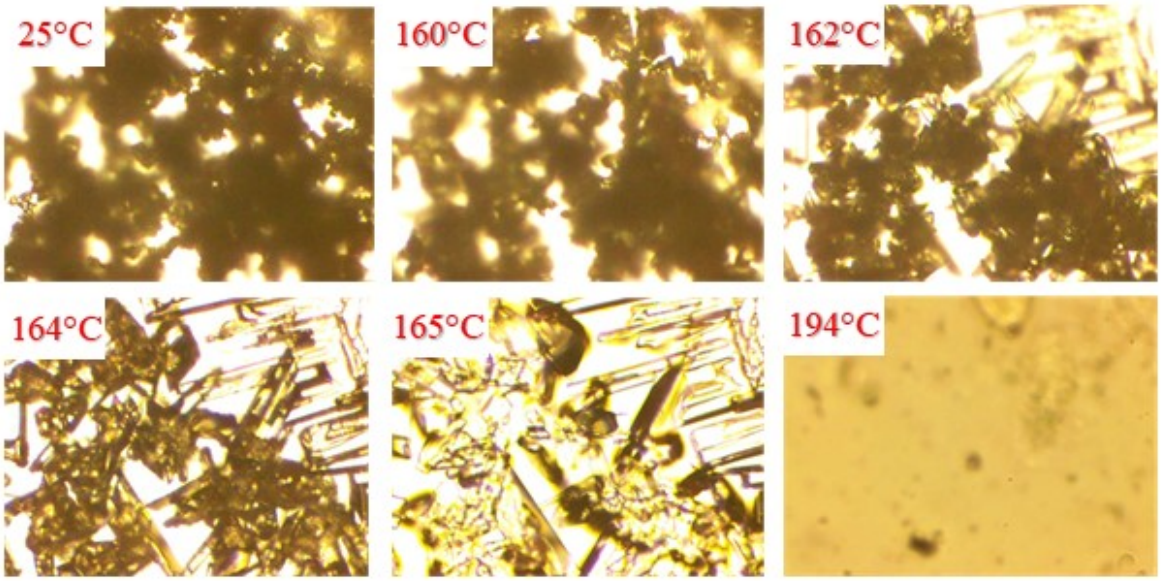

Fig. S2. HSM images of the (NFX+TYA) physical mixture (1:1) taken at various temperatures during the sample heating.

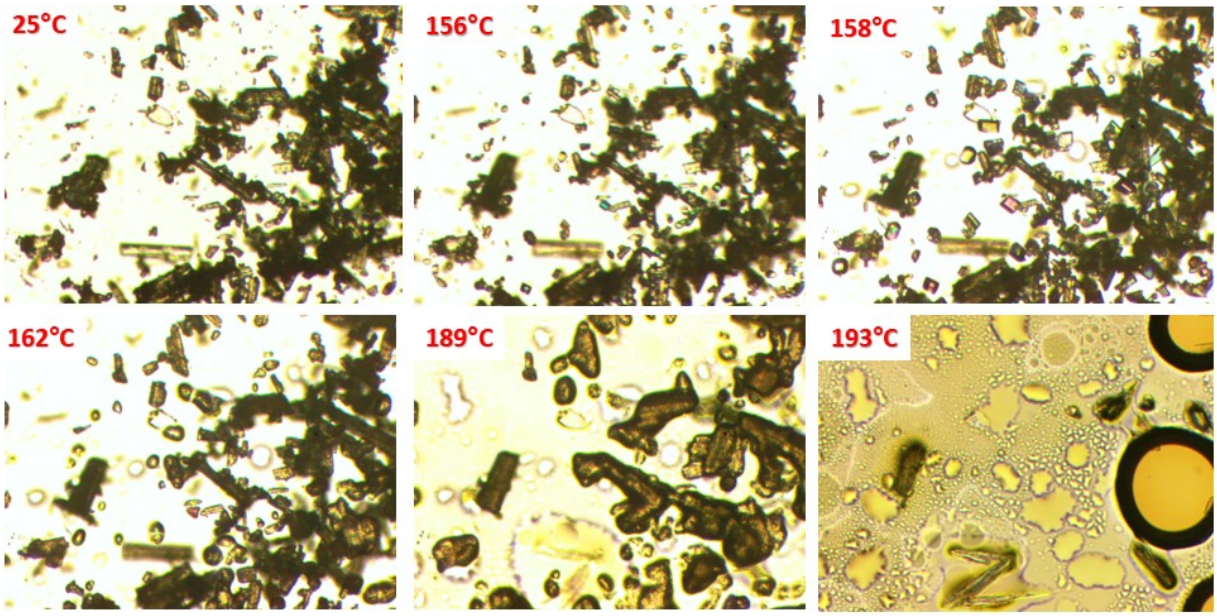

Fig. S3. HSM images of the (LFX+TYA) physical mixture (1:1) taken at various temperatures during the sample heating.

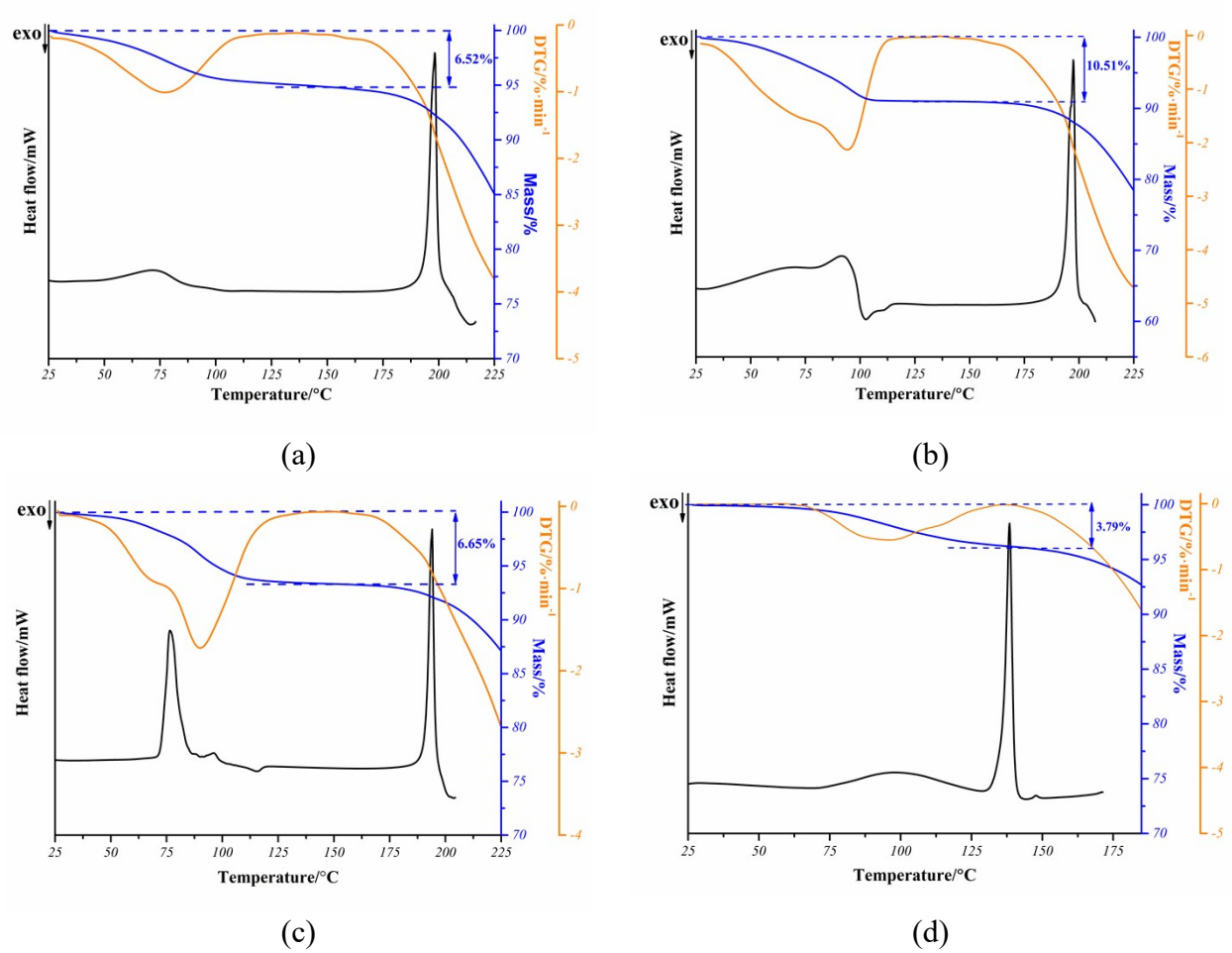

Fig. S4. DSC/TG/DTG curves for: (a) [NFX+TYA+MeOH] (1:1:1); (b) [NFX+TYA+H_2O] (1:1:3); (c) [LFX+TYA+MeOH] (1:1:1) and (d) [EFX+TYA+H_2O] (1:1:1). Expected calculated mass loss for (a) 6.55%; (b) 10.58%; (c) 6.03%; (d) 3.50%

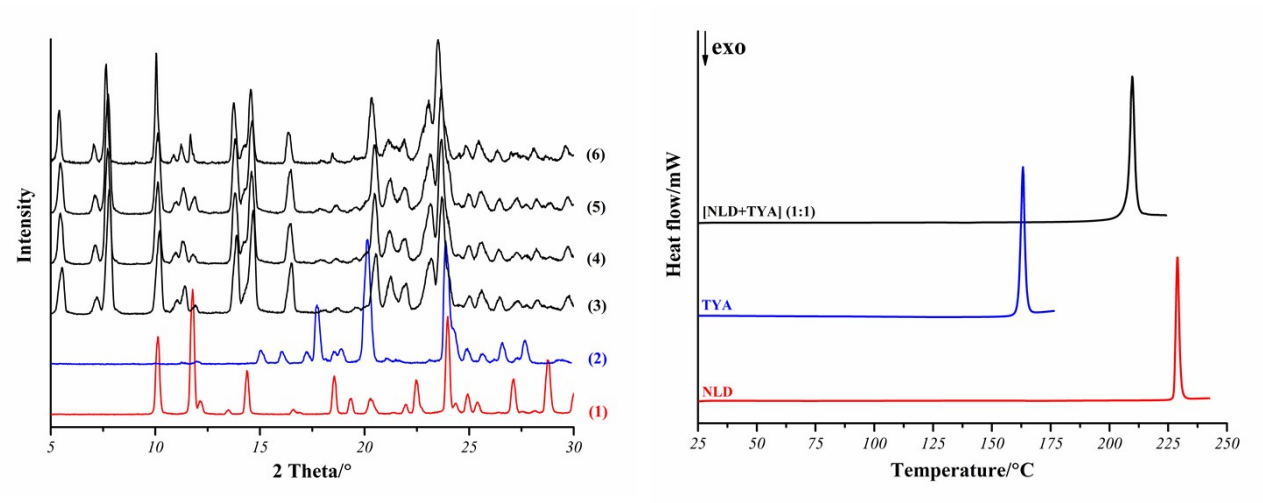

(a) (b)

Fig. S5. (a) Experimental PXRD patterns and (b) DSC curves for mixtures after LAG with different solvents ((1) NLD, (2) TYA, (3) LAG of physical mixture in the presence of EtOH, (4) LAG of physical mixture in the presence of MeOH, (5) LAG of physical mixture in the presence of H_2O, (6) physical mixture (NLD+TYA) (1:1) after heating).

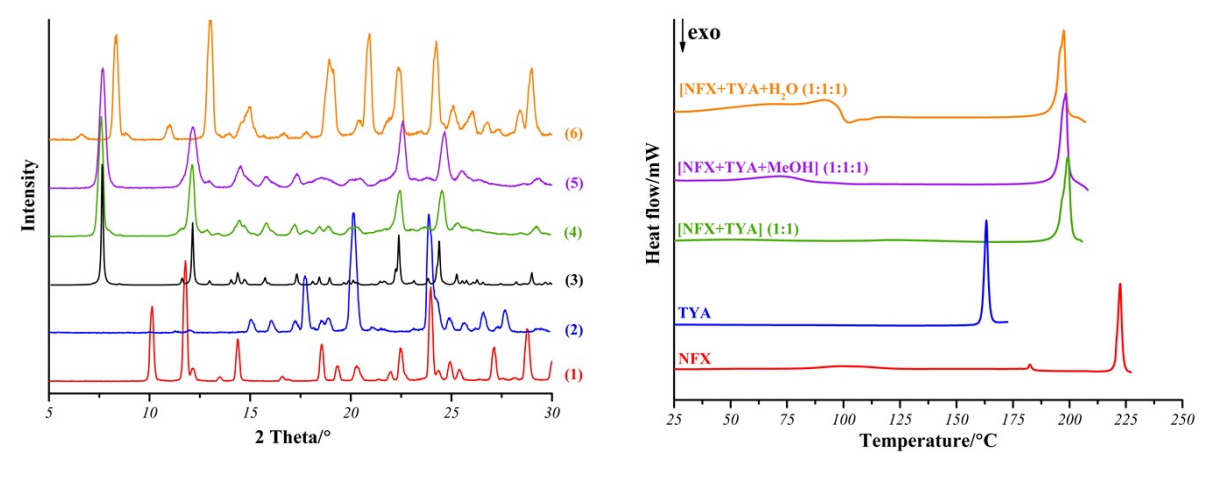

(a) (b)

Fig. S6. Comparisons of (a) PXRD patterns and (b) DSC curves for multicomponent crystals with NFX and TYA ((1) NFX, (2) TYA, (3) [NFX+TYA+MeOH] salt (1:1:1), (4) LAG of physical mixture in the presence of EtOH, (5) LAG of physical mixture in the presence of MeOH, (6) LAG of physical mixture in the presence of H_2O).

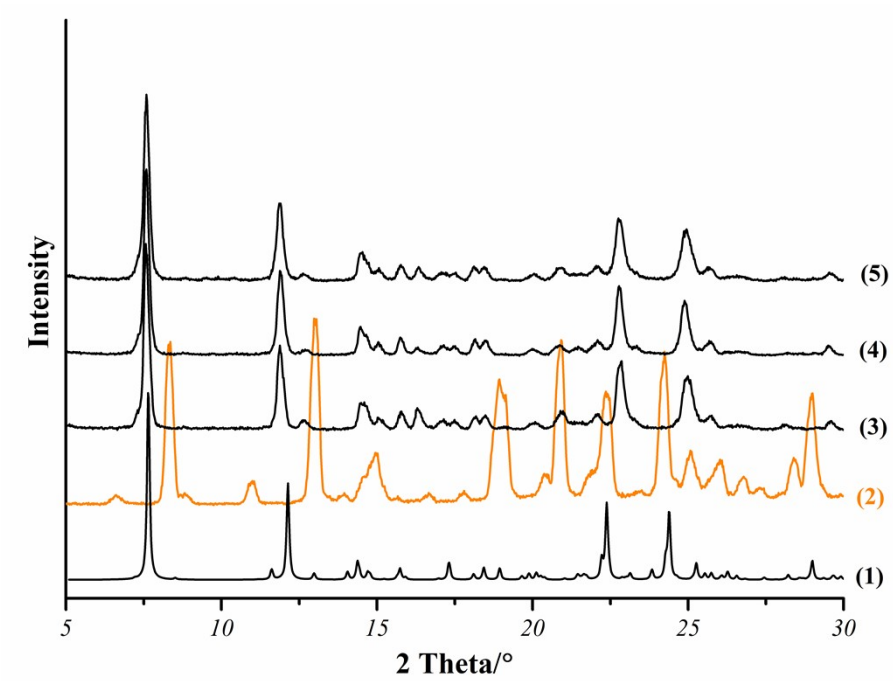

Fig. S7. PXRD patterns for (NFX+TYA) systems (1:1), obtained by thermal methods: (1) [NFX+TYA] (1:1), (2) [NFX+TYA+H_2O] (1:1:3), (3) physical mixture (NFX+TYA) after heating, (4) [NFX+TYA+MeOH] (1:1:1) after heating to 120 °C, (5) [NFX+TYA+H_2O] (1:1:3) after heating to 130°C.

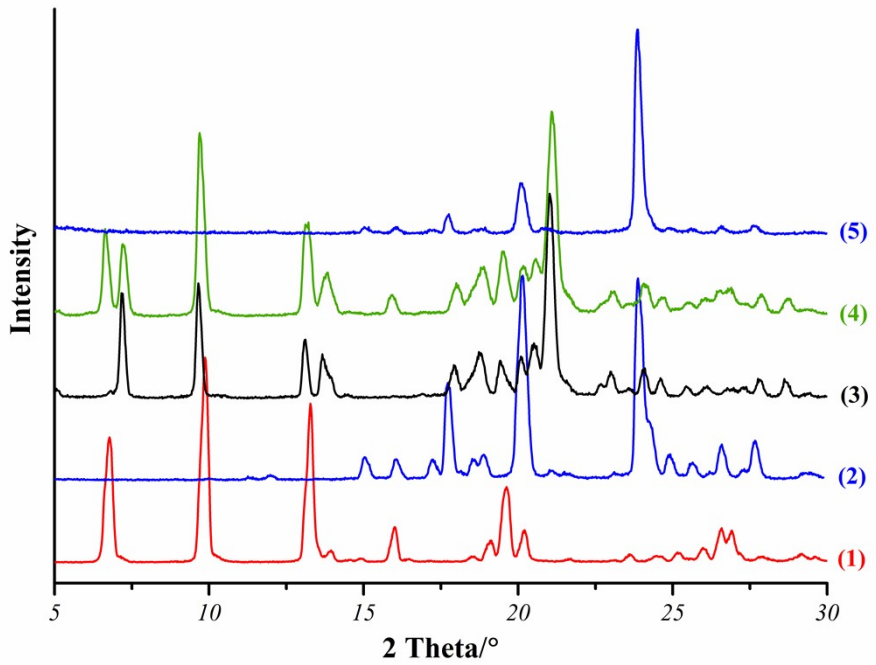

Fig. S8. PXRD patterns of the samples, obtained by (LFX+TYA) (1:1) cosublimation: (1) LFX, (2) TYA, (3) [LFX+TYA] (1:1) Form II, (4) residue phase, (5) sublimate phase.

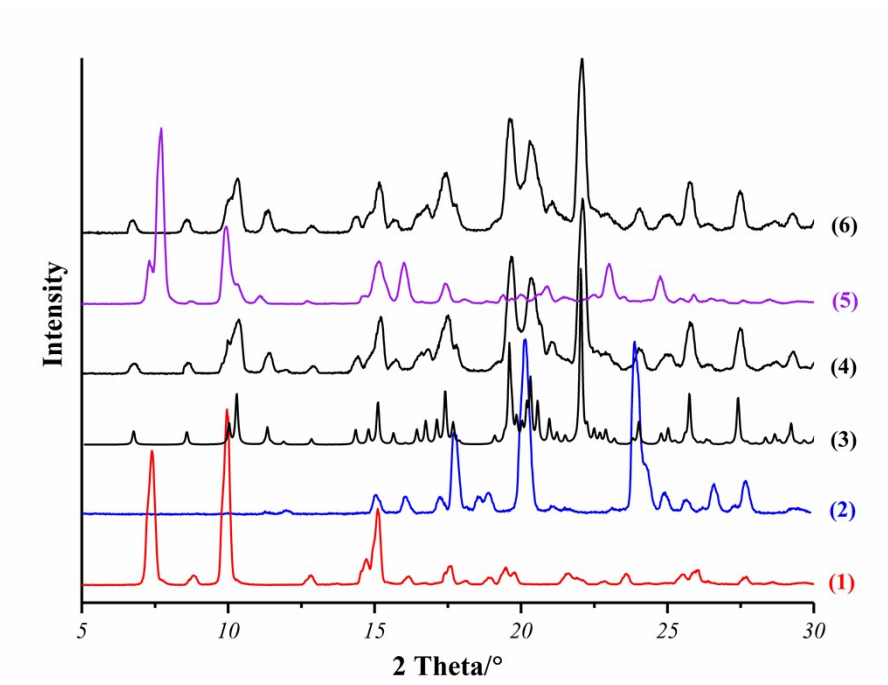

Fig. S9. PXRD patterns of the (EFX+TYA) (1:1) mixtures after liquid-assisted grinding ((1) EFX, (2) TYA, (3) [EFX+TYA+H_2O] (1:1:1), (4) LAG of physical mixture in the presence of EtOH, (5) LAG of physical mixture in the presence of MeOH, (6) LAG of physical mixture in the presence of H_2O).

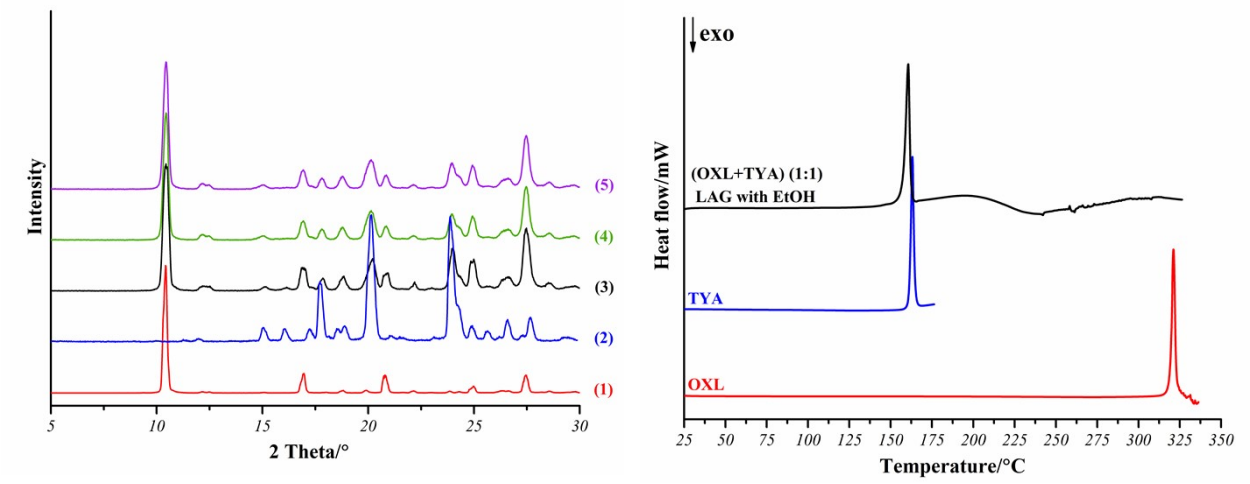

(a) (b)

Fig. S10. (a) PXRD patterns and (b) DSC curves of the (OXL+TYA) (1:1) mixtures, obtained by LAG with different solvents: (1) OXL, (2) TYA, (3) LAG of physical mixture in the presence of EtOH, (4) LAG of physical mixture in the presence of MeOH, (5) LAG of physical mixture in the presence of H_2O.